MARTIAN AEROSOLS IN THE 3µm SPECTRAL RANGE, DURING AND OUTSIDE THE 2018 GLOBAL DUST EVENT BASED ON THE TGO/ACS-MIR CHANNEL.

A. Stcherbinine[1,2], M. Vincendon[1], F. Montmessin[2], M. J. Wolff[3], O. Korablev[4], A. Fedorova[4], A. Trokhimovskiy[4], A. Shakun[4], N. Ignatiev[4], D. Belyaev[4], M. Luginin[4]
[1]Institut d'Astrophysique Spatiale, CNRS, Univ. Paris-Sud, Université Paris-Saclay, 91405 Orsay Cedex, France (aurelien.stcherbinine@ias.u-psud.fr), [2]LATMOS/IPSL, UVSQ Université Paris-Saclay, Sorbonne Université, CNRS, 78280 Guyancourt, France, [3]Space Science Institute, 4750 Walnut Street, Suite 205, Boulder, Colorado 80301, USA, [4]Space Research Institute (IKI), 84/32 Profsoyuznaya, 117997 Moscow, Russia

Introduction: The Atmospheric Chemistry Suite (ACS) instrument from the ExoMars Trace Gaz Orbiter (TGO) ESA-Roscosmos mission started science operation in March 2018 [1,2,3]. The middle-infrared (MIR) channel is a crossed-dispersion echelle spectrometer dedicated to Solar Occultation: each observation covers a 300 nm wide spectral range between 2.3 and 4.2 µm. In this study, we use MIR data acquired before and during the 2018 global dust event to provide constraints about the variability of dust and water ice aerosols associated with the onset and development of the dust storm.

More specifically, we focus on the changes with altitude and time of the 3 µm absorption band of aerosols. This band is related to OH and H_2O molecules absorption: its depth and shape depends on the presence and particle size of water ice [4,5], and is also sensitive to the hydration level of aerosols [6]. We use a dedicated commanding of the instrument centered on the 3.1 – 3.4 µm spectral range.

Water ice clouds monitoring: Since ACS-MIR provides us only 300 nm wide observations, composed of around 20 spectral segments (diffraction orders), we first isolated the spectral continuum and then quantify the 3 µm absorption depth using an Integrated Band Depth (IBD) method [6]. Applying this to all the ACS spectra, we estimate the amplitude of OH/H_2O absorption (that can point to either water ice or hydrated dust) as a function of altitude, for all the observations runs. Figure 1 shows the IBD variations below the haze top in the Southern hemisphere from $L_s = 165°$ and $L_s = 243°$. We observe the presence of two distinct types of vertical profiles, corresponding to the sudden onset of the global dust event ($\sim L_s = 200°$) at theses latitudes (70°S – 80°S) [7].

Before the global dust storm ($L_s < 200°$). During this period, there is a latitude-dependency of the haze top, which increases closer to the equator. The altitude distribution of the water ice clouds seems to follow these variations: the main altitude of clouds detection increases equator-ward (ACS observed latitudes from 64°S to 38°S between $L_s = 165°$ and $L_s = 170°$, and from 24°S to 79°S between $L_s = 180°$ to $L_s = 193°$).

During the global dust storm ($L_s > 200°$). Around $L_s = 200°$, there is a sudden and intense increase of the haze top and water ice particles altitude, without major variation in terms of observed latitude (83°S at $L_s = 196°$ and 74°S at $L_s = 200°$), combined with a decrease of the measured IBD values. In addition, we also note a uniformity around the planet. Specifically,

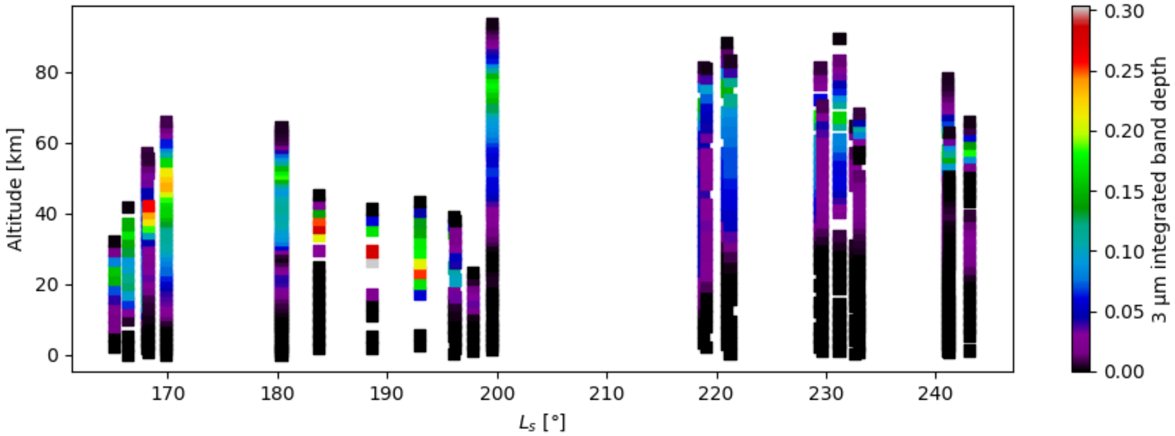

Figure 1 : 3 µm water ice absorption monitoring from the ACS MIR channel occultation in the Martian Southern hemisphere, before and during the 2018 global dust event. The Integrated Band Depth is computed between 3.15 µm and 3.4 µm, on transmitted spectra, below the haze top.

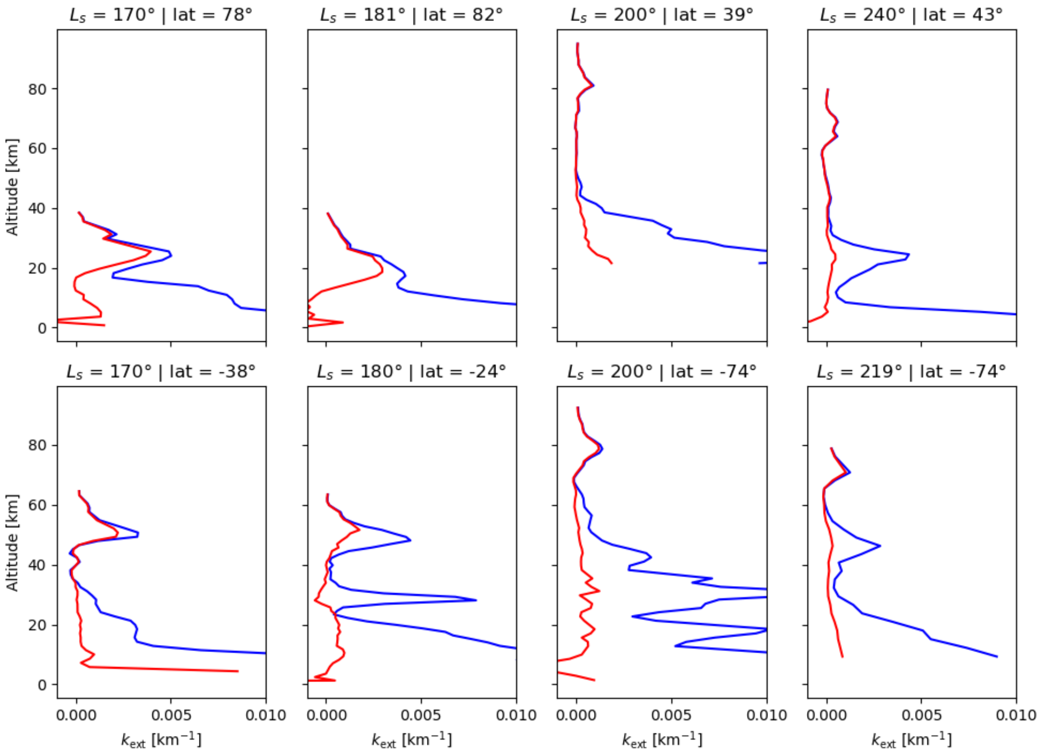

Figure 2 : Extinction coefficient vertical profiles for different ACS-MIR observations. In blue the extinction coefficient at 3.2 µm and in red the difference between the extinction coefficient at 3.2 µm and 3.4 µm.

even though the observed latitude varies from 74°S to 5°S between L_s = 219° and L_s = 241°, one does not see a change in either the haze top altitude or the IBD vertical profile.

Vertical inversion: In order to retrieve the local extinction and properties of the aerosols, we compute a vertical inversion using the onion-peeling method [8], which gives us access to the extinction coefficient k_{ext} of each atmospheric layers. Figure 2 presents verticals profiles of extinction coefficient at 3.2 µm for observations before and during the dust storm. We can see on the one hand that the altitude of the water ice clouds increases during the dust storm, but on the other hand, the k_{ext} associated to the clouds during the dust storm are lower than before. So there is not only a difference between the absorption at 3.2 µm and 3.4 µm as we previously noticed with the IBD, but also a decrease of the extinction at 3.2 µm. Future work will include a modeling of these variations in terms of changes in particle size and optical depth.

Conclusion: We present vertical profiles of water ice clouds in the Martian atmosphere, and the effects of the last global dust storm on them. To this end, we used the data produced by the ACS MIR channel during solar occultations that senses the atmospheric opacity in the 3 µm spectral range. We observe very rapid changes in the aerosol profile associated with the onset of the global dust event, initiating water ice cloud layer formation above 80 km in a period of days or so, suggesting a sudden intensification in the circulation regime. More work is needed to extract more information, such as particle size, yet this preliminary study already provides some insightful data about water ice during the 2018 global dust storm.

Acknowledgments: ExoMars is a space mission of ESA and Roscosmos. The ACS experiment is led by IKI Space Research Institute in Moscow. The project acknowledges funding by Roscosmos and CNES. Science operations of ACS are funded by Roscosmos and ESA. Science support in IKI is funded by Federal agency of science organization (FANO).

References: [1] Korablev et al. (2018) *Space Sci Rev, 214:7*. [2] Korablev et al. (2019) *Nature*, *568*, 517-520. [3] Vandaele et al. (2019) *Nature*, *568*, 521-525. [4] Vincendon et al. (2011) *JGR*, *116*, E00J02. [5] Clancy et al. (2019) *Icarus*, *328*, 246-273. [6] Jouglet et al. (2007) *JGR*, *112*, E08S06. [7] Guzewich et al. (2018) *GRL*, *46*, 71-79. [8] Goldman and Saunders (1979), *JQSRT*, *21*, 155-161.